# Formulation of a porosity operator for joint interpretation of resistivity and microearthquake data across a fluid-filled fracture zone

**Stephen Onacha[1], Peter Malin[2], Eylon Shalev[1], William Cummings[3], Knutur Arnasson[4], and Bjarni Palsson[5]**

.

Total No of pages (Excluding Cover Page) = 6

[1] Department of Earth and Ocean Sciences, Nicholas School of the Environment and Earth Sciences, Duke University, Box 90235, 103 Old Chemistry Building, Durham, N.C 27708-0227
[2] Institute of Earth Science and Engineering, University of Auckland Private Bag 92019, Auckland 1142, New Zealand
[3] Consulting Geophysicist Cummings Geophysics, 4728 Shade Tree Lane, Santa Rosa, CA 95405
[4] Icelandic Geosurvey, ISOR, Orkugardur, Grensasvegi 9, 108 Reykjavik, Iceland
[5] Icelandic National Power Company, Landsvirkjun, Haaleitisbraut 68, 103 Reykjavik, Iceland

# Formulation of a porosity operator for joint interpretation of resistivity and microearthquake data across a fluid-filled fracture zone

**Stephen Onacha[1], Peter Malin[1], Eylon Shalev[1], William Cummings[2], Knutur Arnasson[3], and Bjarni Palsson[4]**

[1] *Department of Earth and Ocean Sciences, Nicholas School of the Environment and Earth Sciences, Duke University, Box 90235, 103 Old Chemistry Building, Durham, N.C 27708-0227*
[2] *Consulting Geophysicist Cummings Geophysics , 4728 Shade Tree Lane, Santa Rosa, CA 95405*
[3] *Icelandic Geosurvey, ISOR, Orkugardur, Grensasvegi 9, 108 Reykjavik, Iceland*
[4] *Icelandic National Power Company, Landsvirkjun, Haaleitisbraut 68, 103 Reykjavik, Iceland*

**Summary -** This paper presents a formulation of a porosity operator that can be used as the basis for joint interpretation of microearthquake and resistivity data across a fluid-filled fracture zone. The use of resistivity and microearthquake measurements is based on theoretical formulation of shared porosity, fluid content and temperature. The relation of resistivity and a double porosity-operator is solved using a basis function. The conceptual model used to formulate the porosity operator over a buried, fluid-circulating fault zone in hydrothermal systems is based on geological and fracture models. The porosity-operator is solved by a basis function and then used to generate a correlation function between P-wave velocity and resistivity. This correlation is then used to generate P-wave velocity and porosity models from 2-D resistivity models generated from magnetotelluric (MT) data through a porosity operator derived from a modified double porosity model.

## 1.0 Introduction

The biggest challenge in the geothermal industry today is to lower the construction time, costs and risks of developing geothermal power plants by drilling fewer high production wells. This can be achieved by developing appropriate methods that map and locate buried fluid-filled faults zones in geothermal systems in different tectonic and geological settings that can be targets for drilling high production wells. One way of reducing costs and risks is to focus research on mapping and characterizing buried fluid-filled fault zones through joint interpretation of seismic and resistivity data.

Geothermal systems are usually found in geologically complex areas that are the foci of intense tectonic and volcanic activity. These processes can produce changes in the rock properties that may be detected by both resistivity and seismic velocity measurements. The tectonic activity coupled with fluid movement in the geothermal systems can produce microearthquake activity. Typically, high-fracture porosity is found at fault tips, fault bends and jogs, and fault intersections. When these structures occur close to geothermal heat sources, they provide important up flow zones. Such zones are excellent targets for exploratory drilling, with the potential to significantly lower the number of wells needed to both delineate a reservoir and place it into economic production. It is known that some geothermal systems for instance Olkaria in Kenya and Krafla in Iceland have some high production wells (Gudmundsson, 2001) that were drilled at the end of production drilling. If these high production wells had been drilled at the beginning of the project, there could have been substantial savings on the infrastructure and the total costs of developing the geothermal power plants.

Resistivity methods have been used in geothermal exploration for many years. Calibration of these methods against drilling results has been done in several geothermal fields, and it is apparent that resistivity measurements can be used as a subsurface thermometer (Arnasson et al., 2000). This indirect spatial correlation between resistivity and temperature is associated with the local degree of hydrothermal alteration. Most high-temperature geothermal systems are associated with a low resistivity layer over the geothermal reservoir due to clay mineral alteration (Arnasson et al., 2000., Flovenz et al., 2005). Resistivity variations are usually related to salinity, water saturation, porosity, and cation exchange capacity in hydrated clays (Ussher et al., 2002. Flóvenz et al., 2005). Understanding the low resistivity distribution and seismic activity can contribute to the location of the high temperature up flow zones as targets for drilling.

## 2.0 Methodology

### 2.1 Conceptual model of a fracture

In this paper, the geophysical and geological model assumes that the porosity within the deep hot geothermal reservoir is dominated by fracture porosity. This is consistent with studies based on the properties of more than 500 samples of igneous rocks in Icelandic hydrothermal systems. These studies show that total porosity is equivalent to effective porosity (Sigurdsson et al., 2000). The data analysis of igneous rock properties in Iceland by Sigurdsson et al. (2000) indicates that matrix permeability is related to the capillary tube model, and therefore, the flow of fluids in the geothermal systems is controlled by fracture porosity, temperature, pressure gradients, and the size and orientation of faults and dykes. Recent studies on core samples from the chlorite zone in geothermal wells in Iceland (Flovenz et al., 2005), found that temperature dependence of conductivity is at least twice as high for interface conduction as for pore fluid conduction. The conclusion is generally that interface conduction is the dominant mechanism for high temperature geothermal fields regardless of fluid salinity (Flovenz et al., 2005).

The conceptual model (Figure 1) used consists of a fault zone, defined as a zone of high fracture porosity which is made up a fracture zone embedded in a host rock. The fault zone is overlain by a clay cap and recent volcanic rocks. The fracture zone is modeled as region of low resistivity while the host rock is modeled as a region of high resistivity.

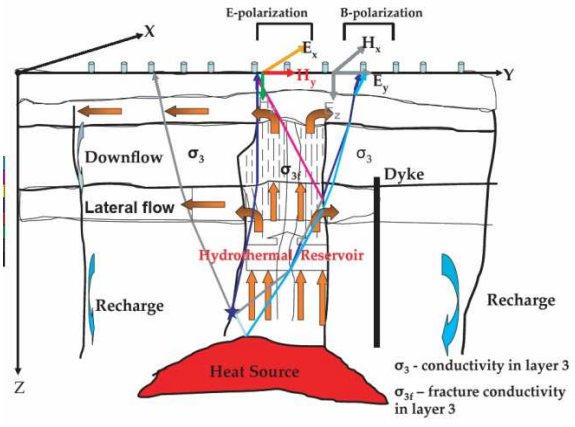


**Figure 1: The conceptual model used for the development of a joint geophysical imaging method using collocated resistivity and earthquake measurements. In this model, the fracture zone is defined by low resistivity and P-wave velocity within a host rock with high resistivity and P-wave velocity. The clay cap occurs above the hydrothermal system and the heat source. Microearthquakes occur above the heat source at the contact between low and high resistivity. Conversions of S-waves to P-waves occur on top of the heat source. The resistivity contrasts below the clay cap cause polarization and splitting in the MT data.**

In general, the conceptual model of the high temperature system close to the fault zone is postulated to have:

1. A surface layer with variable resistivity depending on the age of the rocks and proximity to the fault zone. Areas close to the hydrothermal system are modeled as low resistivity zones formed by the alteration of rocks to low temperature clays. Areas with younger rocks are expected to have higher resistivity.
2. A second isotropic layer with variable thickness formed by alteration of rocks to low temperature clays due to interaction of meteoric water and gases from the deep hot geothermal reservoirs.
3. In high temperature geothermal systems, the third layer is expected to have a higher resistivity due to either a higher degree (chlorite or mixed chlorite and illite) of geothermal alteration or low temperature and fracture porosity. The buried fault zone is postulated to have a lower resistivity due to circulation of geothermal fluids and high fracture porosity.
4. The heat source for the geothermal system has a low resistivity, partially molten magma chamber close to the fault zone.
5. Fluid flow through fractures and stresses on the boundary faults and at the boundary of the heat source and host rock produce microearthquakes. It is postulated that microearthquakes produced above the heat source reflect off on the boundary of the heat source causing conversions of the S-waves to P-waves.

### 2.2 Geological and structural justification for the conceptual model

The geophysical model is based on the geometry of a buried fault zone (Figure 2) within a host rock (Gudmundsson et al., 2002). The fault zone model is based on the observations of systems of mineral veins in the damaged zone of the Husavik-Flatey transform fault zone in northern Iceland with a NW-SE trend (Gudmundsson et al., 2002). The fault zone is about 2-3 km wide and is covered by either volcanic pyroclastic rocks or fresh volcanic rocks, and it is divided into a fault core bounded by damaged zones on either side. The core consists of tectonic gouge and breccias while the damaged zone on either side of the core consists of breccia and fractures of different sizes (Evans et al., 1997).

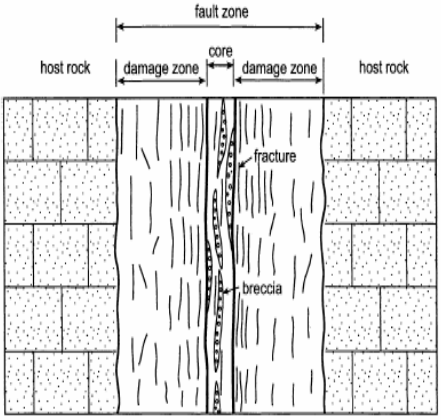


**Figure 2: The structural model of a fault zone showing the core, damaged zone and the host rock. Fault displacement generally occurs either at the core or at the contact with the damaged zone. Fluid flow within the damaged zone can be modeled as flow through a fractured medium (Gudmundsson et al., 2002).**

Intense fracturing can form a zone of high permeability that can allow the flow of geothermal fluids. The contact between the fault zone and the host rock may enhance vertical flow of geothermal fluids by acting as a barrier to deep lateral fluid flow. The assumption is that the fault zone (the size may vary within geothermal systems) is expected to have lower resistivity with the lowest resistivity within the core. The host rock is postulated to have high resistivity and high P-wave velocity.

### 2.3 Formulation of the relationship between resistivity, P-wave velocity and porosity

The theoretical formulation for 1-D and 2-D joint geophysical imaging of fracture zones within geothermal systems can be based on the relationship between resistivity, seismic velocity (both P and S velocities), temperature, fluid saturation, and porosity. In this paper, we propose and develop initial steps of formulating a porosity operator for joint interpretation and inversion MEQ and MT measurements based on shared fracture porosity.

In this paper, we assume that porosity below the clay cap is mainly controlled by fracture porosity. This is based on observations that the formation of zeolites and clays are

dependent on the influx of pore fluid. This process is generally very slow in rock matrix. It is therefore, generally assumed that only fracture porosity contributes significantly towards interface conduction from clays (Flovenz et al., 1985). The total geothermal reservoir storage capacity is therefore a function of the fracture intensity within the fault zone. The general volume average equation that describes the measured resistivity of rocks is shown below:

$$1/\rho = ((1-\Phi_f)(1-P_c))/\rho_b + P_c(1-\Phi_f)/\rho_c + \Phi_d S_w/\rho_w + \Phi_f(1-S_w)/\rho_a \quad 1$$

Where $\rho$, $\rho_b$, $\rho_w$ and $\rho_a$ are the measured resistivity (including fractures), resistivity of rock matrix, resistivity of clay, resistivity of the geothermal fluids (water) and resistivity of air or steam, respectively. $S_w$ is water saturation, $\Phi_f$ is fracture porosity and $p_c$ is percentage of clay. This approach is better than models based on Archie's law which are a good approximation for rocks where the conductivity is dominated by pore porosity only. If we consider the rocks in the geothermal reservoir below the clay cap, and assume maximum fluid saturation and interface conduction by chlorite clays, then the measured resistivity is controlled by porosity in the matrix and fracture porosity, the bulk resistivity and the resistivity of the geothermal fluids. Fracture porosity may be determined from measured resistivity if fluid saturation, clay content, and resistivity of the rock matrix are known. The results of evaluating equation 1 above are compared to those obtained from the double porosity model (that takes into account the matrix and fracture porosity) established by Flóvenz' et al. (1985) for the measured resistivity in Iceland as shown below:

$$\frac{1}{\rho} = \frac{0.22}{\rho_w}\left[1-(1-\Phi_f)^{2/3} + \frac{(1-\Phi_f)^{2/3}}{1+(1-\Phi_f)^{1/3}+(1-\Phi_f)^{1/3}4.9x10^{3}}\right] + \frac{\Phi_f^{1.06}}{b} \quad 2$$

$$\rho_w = \rho_{wo}/\left[1+0.023(T-23)\right] \quad 3$$

$$b = 8.7/\left[1+0.023(T-23)\right]\left[1+0.018(T-23)\right] \quad 4$$

The b factor is temperature dependent and relates average fracture density over large volumes of rock to the interface conductivity and fracture porosity (Flovenz et al., 1985). This model also takes into account the effect of temperature and pore fluid. The model also takes into account conduction through the fracture interfaces. The first step is to empirically analyze and formulate the dependence of pore water resistivity on temperature using equation 3 which indicates that for a reservoir saturated with meteoric water with a low percentage of dissolved salts, the pore water resistivity would be expected to be close to that of water at room temperature which is about 2.5 x105 Ωm at 23˚C. The results show that the resistivity of fresh water does not significantly reduce with increase in temperature.

The resistivity of the geothermal fluids can also be determined from laboratory measurements or from the geochemical data by using the total dissolved solids (TDS) in g/l using the empirical relationship by Block, (2001) as shown below:

$$\rho_w = 4.5TDS^{-0.85} \quad 5$$

For instance, at the Krafla geothermal system, the average TDS is about 800 ppm, which is equivalent to 0.8 g/l. This translates to a pore water resistivity of about 5.4 Ωm. In comparison, sea water has a TDS of about 30 g/l, which gives an equivalent pore water resistivity of 0.25 Ωm. From equation 2 above, the measured resistivity will strongly depend on the resistivity of the pore fluid.

An important step in determining the relationship between resistivity and porosity involves empirically evaluating the dependence of b in equation 4 on temperature (Figure 3). The plot shows that the value of b is higher and changes more rapidly at low temperatures below 150˚C. For high reservoir temperatures (>200˚C), the value of b is low and changes very gradually. This empirical relation can therefore be used to determine the value of b in equation 2.

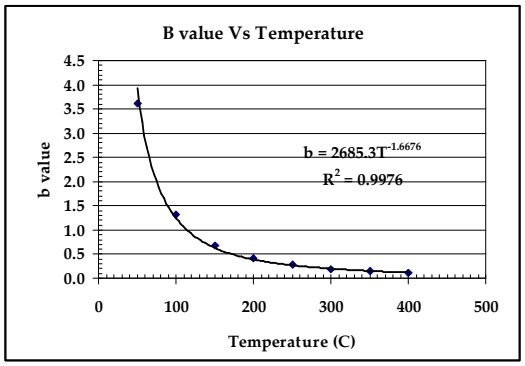


**Figure 3: Plot of the constant b value in equation 2.6 for a temperature range of 50-400°C. The change in the b values are higher at low temperatures and very small at high temperatures (>200).**

The limiting values of the dependence of resistivity on porosity can be qualitatively analyzed by considering two cases of fracture porosity. The first case is when the fracture porosity is very small, and the second case is when fracture porosity is dominant. In the first case, when fracture porosity is very small, the measured resistivity depends only on the resistivity of the geothermal pore fluid. This means that when fracture porosity is very small, the measured resistivity for rocks is then expected to be very high. When fracture porosity is very high (totally fractured and saturated rock), the measured resistivity is both a function of fluid resistivity and the b factor

Equations 1 and 2 can be rearranged as shown below to solve for porosity using a basis function. The basis function finds a point with a value near zero as the solution for the resistivity equation to solve for the fracture porosity of the rocks given the range of the resistivity of the formation, the resistivity of the geothermal fluid at reservoir temperature, very low percentage of clay, and fully saturated rocks. The basis porosity functions are expressed as shown below:

$$f(\Phi) = \frac{(1-\Phi)(1-P_c)}{\rho_b} + \frac{Pc(1-\Phi)}{\rho_c} + \frac{\Phi S_w}{\rho_w} + \frac{\Phi(1-S_w)}{\rho_a} - \frac{1}{\rho} \quad 6$$

$$f(\Phi) = -\frac{1}{\rho} + \frac{0.22}{\rho_w}\left[1-(1-\Phi_f)^{2/3} + \frac{(1-\Phi_f)^{2/3}}{1+(1-\Phi_f)^{1/3}+(1-\Phi_f)^{1/3}4.9x10^{-3}}\right] + \frac{\Phi_f^{1.06}}{b} \quad 7$$

The basis function tries to find a zero of the equation with one variable, in this case porosity, with a specified starting interval between 0.0001-0.9. The algorithm uses a combination of bisection, secant, and inverse quadratic

interpolation methods to determine porosity. The basis function can be evaluated for both equation 6 and 7. In equation 6, a solution was found for values of a percentage of clay at about 10 percent, matrix resistivity of 5,000 Ωm (which is the estimated value for resistivity of a basaltic rock), and resistivity of clay at about 5 Ωm, and water resistivity of 7 Ωm. When the percentage of clay is very high or resistivity of clay is less than 5 Ωm, then the solution gives very high values of porosity. The high values obtained for porosity show that the model cannot be explained by fracture porosity in areas dominated either by clays or very low resistivity where ionic conduction is dominant.

Analysis of the results from equations 6 and 7 indicates that equation 7, which takes into account the effect of temperature, might underestimate the porosity determined from some cores in the geothermal fields. From the analysis of the resistivity and porosity from equation 7, the value of

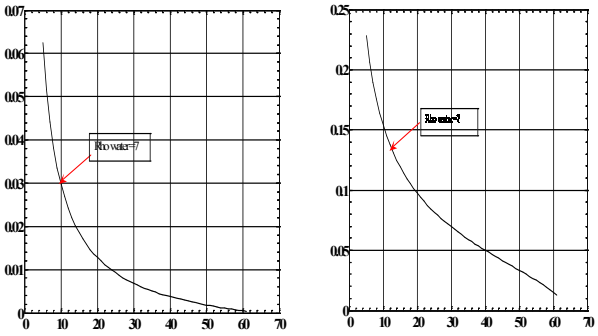


fracture porosity obtained is less than 10% (Figure 4) and is not consistent with porosity data from the geothermal systems.

**Figure 3: Plots of fracture porosity determined from equation 2.11shown on the left and fracture porosity determined from a modified equation 6 with a higher exponent for the fracture porosity shown on the right. Fracture porosity determined from equation 7 is very low (<10%).**

From this analysis, there is a very narrow range (5-130 Ωm) of resistivity that correlates with high fracture porosity of more than 5%. The fracture porosity is very low for resistivity more than 130 Ωm. We have then assumed that the areas with high resistivity at a depth of more than 1000m have low fracture porosity and possibly low reservoir temperatures. These limits for resistivity are used in the objective function to formulate the relationship between resistivity and P-wave velocity based on the porosity distribution derived from resistivity.

When the exponent of fracture porosity is modified from 1.06 to a value greater than 2 in equation 7, the solution gives consistent results with the measured effective porosity of between 0% and 50% with porosity as high as 49% measured in the igneous samples with the majority falling below 20% (Sigurdsson et al., 2000).

Based on this analysis equation 7 has been modified with a higher exponent and used to determine the relationship between resistivity and porosity (Figure 6) using the equation shown below.

$$f(\Phi)=-\frac{1}{\rho}+\frac{0.22}{\rho_w}\left[1-(1-\Phi_f)^{2/3}+\frac{(1-\Phi_f)^{2/3}}{1+(1-\Phi_f)^{1/3}+(1-\Phi_f)^{1/3}4.9x10^{-3}}\right]+\frac{\Phi_f^{\,2}}{b} \qquad 8$$

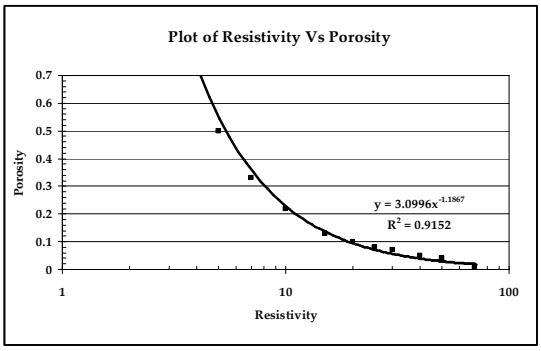


**Figure 4: Plot of resistivity against porosity derived from solving a basis function for a double porosity model relating porosity to resistivity close to the fracture zone.**

The relationship between porosity $(\Phi_f)$ and resistivity $(\rho)$ is shown below:

$$\Phi_f = 3.0996\rho^{-1.1867} \qquad 9$$

The porosity and resistivity relationship described above can be used to formulate the relationship between P-wave velocity and resistivity. In fields where porosity has been determined, the results can be compared and the basis function re-evaluated to match field properties. For instance, when the empirically determined values of porosity are compared with those measured in the geothermal systems in Iceland and Kenya, the modified double porosity model gives a good estimate of the observed porosity. The porosity values are similar to those obtained from cores in the Olkaria geothermal field in Kenya. The porosity values range from 0% to 45% with most samples having porosity of 5-20%. This therefore justifies the use of a higher exponent for equation 8 to generate the fracture porosity for various geothermal systems.

### 2.4 Relationship between P-wave velocity, porosity and resistivity

When an earthquake is generated, body waves travel through the rocks. The main interest is in the body waves which generate P-waves and S-waves which are related to the elastic coefficients mainly the bulk density, shear and bulk modulus. The bulk density $\rho_b$ depends on fracture-porosity $\Phi_f$, density of the rock matrix $\rho_m$ and density of the fluid $\rho_f$ as shown below:

$$\rho_b = \Phi_f \rho_f + (1-\Phi_f)\rho_m \qquad 10$$

In geothermal systems, the density of the fluid is a function of temperature, salinity and pressure. The P-wave velocity and porosity relationship has been established based on the equation by Wyllie et al., 1958 shown below:

$$\frac{1}{V_p}=\frac{\Phi_f}{V_w}+\frac{1-\Phi_f}{V_r} \qquad 11$$

where $V_p$ is the bulk P-wave velocity, $V_w$ is the P-wave velocity in water, $V_r$ is the P-wave velocity of the rock matrix, and $\Phi_f$ is the fracture porosity. If the velocities of the

geothermal fluid and that of the un-fractured rocks are known, the Wyllie equation can be used to solve for porosity. If we assume that for the case of Krafla, the P wave velocity of the basalt is about 6000ms-[1]and the velocity of water is 1500 ms-[1], the relationship between porosity and P-wave velocity based on the Wyllie equation can be expressed as shown below:

$$\Phi_f = 2000ms^{-1}V_p^{-1} - 0.33 \qquad 12$$

By combining equations 8 and 11, and if the fracture porosity and the resistivity of the fluid are known, then P-wave velocity can be calculated. From the analysis of the relationship between resistivity and porosity, we propose that in areas with resistivity high than 130 Ωm the fracture porosity is very low, and therefore from equation 11, the P-wave velocity approaches that of the rock matrix. It is therefore expected that the variation in porosity is significant only in areas with low resistivity close to the fracture zone. As an example, when the measured resistivity is about 10 Ωm, the porosity about 15% and equation 11 can be expressed as

$$0.15 = 2000ms^{-1}V_p^{-1} - 0.33 \qquad 13$$

$$V_p = \frac{2000ms^{-1}}{0.48} = 4167\ \mathrm{ms}^{-1} \qquad 14$$

This value is consistent with expected acoustic P-wave velocity of 4000-4600 m/s for basaltic samples with grain densities higher than 3000 kg/m3 (Sigurdsson et al., 2000).

### 2.5 Resistivity operator

The relationship between resistivity, P-wave velocity and porosity has been used to define a porosity operator as shown below.

$$f(\Phi_f) = \begin{Bmatrix} 0 & \rho \geq 130\Omega m & V_P \geq 6000ms^{-1} \\ 0.5-0\cdots 5 \geq \rho \leq 130\Omega m\ldots & 2500 \geq V_P \leq 6000ms^{-1} \\ 1-0.5 & 0 \geq \rho \leq 5\Omega m & V_P \leq 2500ms^{-1} \end{Bmatrix} \qquad 15$$

The initial porosity model parameters are estimated by solving the basis function for the relationship between resistivity and porosity by using the limits defined in equation 8 and 15 to generate the P-wave velocity. The relationship between P-wave velocity and resistivity is given by:

$$V = 776.15 + 471.6\rho - 19.3\rho^2 + 0.3382\rho^3 - 0.002\rho^4 \qquad 16$$

The relationship between porosity and P-wave velocity taking into account the approximation in equation 8 is given as

$$\Phi_f = 0.0021V - 8\times10^{-7}V^2 + 10^{-10}V^3 - 6\times10^{-15}V^4 - 1.3238 \qquad 17$$

The formulated resistivity operator close to a fracture zone can be used to generate P-wave velocity models for locating earthquakes. The 1-D model obtained by this method in the Krafla geothermal field compares very well with the existing models (Brandsdottir et al., 1997). The main difference is at depth, where previous models assumed that velocity generally increases with depth. The advantage of this approach is that usually a large number of electrical resistivity data exists in many geothermal fields.

The porosity operator can also be used to develop a joint inversion of microearthquake and resistivity data (Onacha 2006). In this formulation, we propose that the inversion can be solved through a defined objective function, which takes into account the factors that relate both resistivity and P-wave velocity to porosity in the vicinity of a fracture zone in a geothermal system. Fracture porosity, determined from resistivity and seismic waves can be related through an operator similar to that defined by Haber and Oldenburg (1997) such that:

$$\Im_R[m_R] = d_R \quad \text{and} \quad \Im_S[m_S] = d_S \qquad 18$$

where the subscripts R and S refer to resistivity and seismic waves, $\Im$ is the operator representing measurements, $m$ represents the model parameters and $d$ represents data. For 2-D, the model parameters are expressed as grids with different porosities. The assumption is that the porosity is constant in each grid. The data for joint inversion are MT resistivity and P-wave velocity for MEQ.

## 3.0 Results

In this paper, the porosity operator is used to define the porosity and P-wave models generated from resistivity data. The porosity operator was used together with the 2-D resistivity grid (Figure 5) to generate porosity (Figure 6) and P-wave velocity (Figure 7) models. The objective is to show that the porosity image generated has the same structure as the resistivity model. This approach will be developed further into a joint inversion scheme.

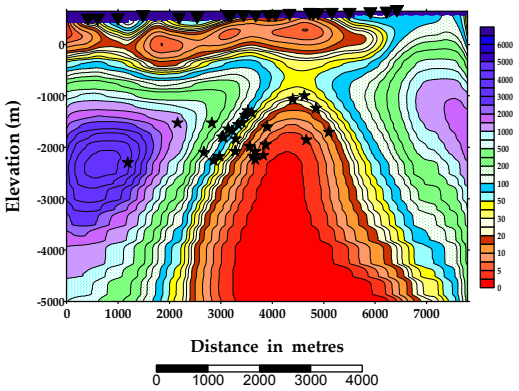


**Figure 5: Plot of 2-D resistivity model for profile NE1 to the northern part of Krafla. The earthquakes occur on the boundary of the low and high resistivity above the interpreted heat source. The near surface low resistivity defines the cap rock.**

## 4.0 Discussions

The near surface high porosity corresponds to a region with low-temperature clays due to lateral movement of hydrothermal fluids. The low porosity corresponds to areas with high resistivity. The areas with high resistivity show low porosity while areas with low resistivity show high porosity. We note that the values of porosity obtained have high errors (20%) because MT models have a better resolution of conductance rather than resistivity. The emphasis in this paper is on the contrasts rather than the obsolete values

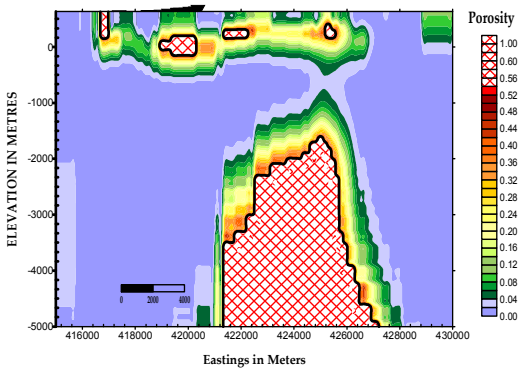


**Figure 6: Porosity model generated from 2-D resistivity model. The highest fracture porosity occurs within an interpreted fracture zone.**

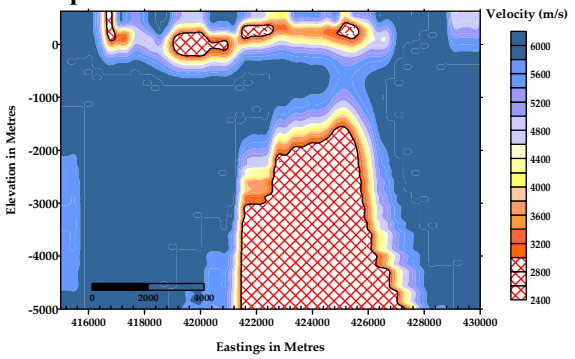


**Figure 7: P-wave velocity model generated from 2-D resistivity inversion model. The lowest P-wave velocity occurs within a narrow area interpreted as a fracture zone. The near surface P-wave resistivity corresponds to a region with low-temperature clays due to lateral movement of hydrothermal fluids. The high P-wave velocity corresponds to areas with high resistivity and low porosity.**

Although areas with resistivity less than 5 Ωm are shown as having high porosity, they only represent areas where the porosity operator is dependent of the high clay content and therefore not a reliable representation of the fracture model. In this case, the shallow areas with intermediate resistivity correspond to the clay cap. The deep low resistivity is associated with the interpreted partially molten heat source. The areas with low P-wave velocity and low resistivity less than 5 Ωm are interpreted as regions with either high clay alteration or high-temperature partially molten rock interpreted as the heat source for the hydrothermal system. The good correlation between resistivity and temperature measurements shows that the deeper low resistivity zones are associated with high permeability and temperature. The porosity maps therefore give an indication of areas that could be targets for drilling high production wells.

## 5.0 Conclusions

- This paper demonstrates that resistivity data can be used to generate P-wave velocity and porosity from a porosity operator.
- We propose the use of the porosity operator to carry out a joint inversion of resistivity and microearthquake data by minimizing an objective function.
- Resistivity can be used to generate P-wave velocity independent from that generated by ray tracing.
- Fracture porosity imaged by the resistivity double porosity modeling varies between 5-45%. The porosity is highest in an interpreted fracture zone.


## ACKNOWLEDGEMENTS

We are grateful to Duke University, Kenya Electricity Generating Company (KenGen), DOE, the Icelandic National Power Company (Landsvirkjun), and Icelandic Geosurvey (ISOR) for the support for this work.


## References


Arnasson, A., Ragna, K., Hjalmar, E., Flovenz, O., and Steiner G. (2000). The resistivity structure of high temperature geothermal systems in Iceland. Proceedings of the world geothermal congress, Kyushu Japan, 923-928.

Block, D. (2001). Water Resistivity Atlas of Western Canada. , Rock Foundation Convention of the Canadian Society of Petroleum Geologists. Calgary, Canada.

Brandsdottir, B., Menke, W., Einarsson, P., White, R., and Staples, R. (1995). Crustal structure of the Krafla central volcano in the northern volcanic zone of Iceland as determined through seismic observations. Reykjavik: Science Institute, University of Iceland.

Evans, J., Forster C., and Goddard, J. (1997). Permeability of fault-related rocks, and implications for hydraulic structure of fault zones. J. Struct. Geol., 19, 1393-1404.

Flovenz, O., Spangenberg, E., Kulenkampff, J., Arnason, K., Karlsdottir, R., and Huenges, E. (2005). The role of Electrical conduction in geothermal exploration. Paper presented at the World Geothermal Congress, Antalya, Turkey.

Flovenz, O. G. (1985). Application of subsurface temperature-measurements in geothermal prospecting in Iceland. Journal of Geodynamics, 4(1-4), 331-340.

Gudmundsson, A. (2001a). An expansion of the Krafla power plant from 30 to 60 MWe Paper presented at the Geothermal Resources Council Transactions.

Gudmundsson, A., Fjeldskaar, I., and Brenner, S. (2002). Propagation pathways and fluid transport of hydrofractures in jointed and layered rocks in geothermal fields. Journal of Volcanology and Geothermal Research, 116(3-4), 257-278.

Onacha, S.A. (2006). Hydrothermal fault zone mapping using seismic and electrical measurements. Ph.D Thesis, Duke University pp225

Sigurdsson, O., Gudmundsson, A., Fridleifsson, O., Franzson, H., Gudlaugsson, S., and Stefansson, V. (2000, May 28-June 10). Database of igneous rock properties in Icelandic geothermal systems: Status and unexpected results. Paper presented at the World Geothermal Congress, Kyushu-Tohuku, Japan.

Ussher, G., Harvey, C., Johnstone, R., and Anderson, E (2000, May 28- June 10). Understanding the resistivity observed in geothermal systems. Paper presented at the World Geothermal Congress, Kyushu-Tohoku, Japan.

Wyllie, R., Gregory, A., and Gardner, G. (1958). An experimental investigation of factors affecting elastic wave velocities in porous media. Geophysics, 23, 459-493.